The impact of increased atmospheric carbon dioxide on microbial community dynamics in the rhizosphere

Drigo, B.

Chapter 6

Distinct root-associated communities are selected by elevated atmospheric CO_2

Barbara Drigo, Agata S. Pijl, Anna M. Kielak, Hannes Gamper, Paul L.E. Bodelier, Andrew S. Whiteley, Johannes A. van Veen and George A. Kowalchuk

Results of chapter 5 and 6 submitted to Nature (see Intermezzo).

Abstract

Rising atmospheric CO_2 levels are predicted to have major consequences upon carbon cycle feedbacks and the overall functioning of terrestrial ecosystems. Photosynthetic activity and the structure of terrestrial macrophytes, especially C_3 plants, are expected to change, but it remains uncertain how this will affect soil-borne communities, which are dependent on plant-derived carbon, and their feedbacks on ecosystem function. Using a controlled growth system, we examined the impact of elevated atmospheric CO_2 on soil-borne microbial communities by comparing belowground community responses associated with plants grown under ambient (350 ppm) versus double ambient (700 ppm) CO_2 environments. The combination of RNA-based stable isotope probing (SIP), community fingerprinting analysis and real-time PCR allowed us to trace plant-fixed carbon to the affected soil-borne microorganism. Here, we demonstrate that elevated atmospheric CO_2 selects for distinct microbial populations incorporating plant-derived carbon. As opposed to simply increasing the activity of soil-borne microbes resident at ambient CO_2 conditions, elevated atmospheric CO_2 strongly selects for opportunistic plant-associated microbial communities, with a particular shift in the dominant arbuscular mycorrhizal fungi community as well as rhizosphere bacterial and fungal populations.

Introduction

Although it has been clearly been established that anthropogenic CO_2 emissions are contributing to rising atmospheric CO_2 levels, the rate of atmospheric CO_2 elevation remains uncertain (IPCC, 2007). A major contribution to this uncertainty is our lack of knowledge of climate-carbon cycle feedbacks related to vegetated terrestrial ecosystems. The biogeochemical carbon (C) cycle is greatly influenced by terrestrial macrophytes, which provide a path for movement of C via their roots to the largest and most stable C pool in the terrestrial biosphere, the soil. Many field studies have found that elevated CO_2 concentrations lead to higher C assimilation by plants (Ainsworth & Long, 2005). Subsequently, a substantial portion of this "extra" C fixed by plants enters the soil organic C pool in the soil by direct deposition to soils, through an increased turnover of roots, by increased biomass of sloughed-off cells, enhanced plant tissue breakdown or increased root exudation (Zhou *et al.* 2006; Pendall *et al.* 2004). The C substrates entering the soil typically undergo rapid metabolism by soil-borne microorganisms. Because the decomposition of plant photosynthates by root microorganisms is key to the terrestrial C budget, the response of photosynthesis to elevated atmospheric CO_2 will strongly impact soil C dynamics (Korner & Arnone, 1992).

The structure of soil-borne prokaryotic communities is known to be affected by plant species and nutritional status (Garbeva *et al.* 2004; Smalla *et al.* 2001; Kowalchuk *et al.* 2002). Therefore, it is expected that soil-borne microbial communities will respond to elevated atmospheric CO_2 via changes in plant photosynthesis levels and physiology. Rhizosphere bacteria and arbuscular mycorrhizal fungi (AMF) have been postulated to be the most important sequesters of plant-derived C in plant-soil systems (Staddon, 2005; Phillips, 2007). Mycorrhiza play a distinct and unique role in C sequestration by immobilizing C in living fungal tissues and by producing recalcitrant compounds that remain in the soil following fungal senescence (Rillig *et al.* 2001; Treseder *et al.* 2007). In addition, mycorrhizal fungi contribute indirectly to soil organic C (SOC) stabilization via their role in the formation and stabilization of soil aggregates (Rillig & Mummey, 2006).

Lastly, mycorrhizal fungi are hypothesized to further enhance C sequestration by translocating nutrients from the bulk soil to the host plant, thereby competing with free-living decomposer microorganisms that would otherwise mineralize soil organic C to CO_2 (Rillig & Allen 1999). In the context of global environmental change, mycorrhizal fungi may, therefore, play a central role in the biogeochemical C cycle and responses to rising CO_2 levels (Staddon, 2005).
In order to track the fate of plant-assimilated C to the belowground microbial community, and to examine the impact of elevated atmospheric CO_2 levels on these processes, we conducted a $^{13}CO_2$ pulse-chase labelling experiment. The controlled growth model system involved a endomycorrhizal perennial C_3 plant species, *Festuca rubra* ssp. *arenaria* and examined microbial community responses associated with plants grown under ambient (350 µl/l) versus elevated (700 µl/l) CO_2 conditions. In previous experiments, we observed significant shifts in the rhizosphere microbial community of *F. rubra* upon growth at elevated atmospheric CO_2 concentrations (see chapters 4 and 5). Here, we used a combination of RNA Stable Isotope Probing (RNA-SIP) (Radajewski *et al.* 2000; Manefield *et al.* 2002), community fingerprinting analysis and qPCR to facilaite the *in situ* identification of microbial populations affected by elevated CO_2 concentrations. Analyses targeted total bacterial, total fungal, *Pseudomonas* spp., *Burkholderi*a spp. and AMF communities, and the resulting data are examined in the light of potential impacts of elevated CO_2 on plant-microbe interactions.

Methods

Soil collection, plant pretreatment conditions, ^{13}C pulse-labeling and the harvesting procedures for *Festuca rubra* were as previously described in chapter 5. Briefly, soil was collected at Bergharen (the Netherlands), sieved, homogenized and wetted to 10% volumetric water content. A total of 200 four week-old *F. rubra* seedlings were grown in this soil for 180 days in controlled growth cabinets, half at ambient (350 µl/l) and half at elevated (700 µl/l) atmospheric CO_2 concentrations. For each CO_2 treatment, 96 plants, plus 16 unplanted pots were subjected to $^{13}CO_2$ pulse-labeling 181 days after seedlings were planted (211 total growing days).

Isotope ratio mass spectrometry (IRMS)

Actual ^{13}C-content (excess ^{13}C) in different plant-soil fractions (shoots, roots, soil) was calculated as described in Boschker (2004). A sample of the remaining roots and rhizosphere soil was dried. The ^{13}C-enrichment in root and soil samples, reported in $\delta^{13}C$ ‰ ($^{13}C/^{12}C$ ratio), was calibrated to the internal gas standards and solid reference against Pee Dee Belemite standard. All isotopic signatures ($\delta^{13}C$) were determined by continuous flow combustion isotope ratio mass spectrometry. The isotopic composition of the lipid fractions was determined on a gas chromatograph (Hewlett Packard HP G1530) coupled to a Thermo Finningan Delta-plus IRMS via a type III combustion interface (GC-C-IRMS), and the results are described in chapter 4 (Fig. 3).

Extraction and analysis of DNA and RNA

Rhizosphere soil was defined as the soil that remained attached to roots after removal from pots and gentle shaking. Remaining soil was defined as bulk soil. Subsequently, the rhizosphere soil was carefully removed from the roots with a probe and forceps. Root fragments remaining in the bulk or rhizosphere soil samples were removed by passing through a 1-mm sieve. After additions of RNA Stabilizating Reagent according to manufacture's protocol (RNAlater, Qiagen), all soil samples (rhizosphere, bulk and unplanted) were frozen immediately following harvest with liquid nitrogen and stored at -80 °C until DNA and RNA extraction. From sampling until cDNA synthesis, all RNA handling was performed under RNAse-free conditions. Aqueous solutions were treated with 0.1% diethyl pyrocarbonate (DEPC). Glassware was heated to 200 ºC overnight and plastic material soaked overnight in 0.1 N NaOH/1 mM EDTA solution, before rising with RNAse-free water. The working area and materials reserved for RNA handling were treated with RNAse decontamination solution (RNase*Zap*®, Ambion). Total RNA was extracted using a modified method of Griffiths *et al.* (2000). 0.5 g of rhizosphere soil (wet weight) was weighed out into 2 ml tubes, and nucleic acids were extracted by bead-beating with a mix of 0.5 and 0.1 mm zirconia/silica beads (Merlin Bio products, The Netherlands) with CTAB/phosphate buffer and phenol-chloroform-isoamyl alcohol extraction (PCI, 25:24:1 (vol/vol/vol), Ambion). Nucleic acids were precipitated using two volumes of 30% PEG (6000)/1.6 M NaCl and incubated overnight at +4 ºC. Following centrifugation (20000×*g*), pellets were washed with 70 % ethanol and resuspended in 50 µl of RNAse-free water (Fermentas). RNA was prepared from the primary extracts by digestion of co-extracted DNA with RNAse free DNAse (Quiagen) according to the manufacture's protocol. The integrity of the RNA preparations was visualized by LabChip® microfluidic technology and automated electrophoresis for RNA analysis using the Experion RNA StdSens analysis system (Experion™, Bio-Rad Laboratories Inc., the Netherlands) and subsequently store at -80 ºC. Total RNA was quantified using both the Experion™ system and a NanoDrop, ND-1000 Spectrophotometer (Bio-Rad Laboratories Inc., the Netherlands).

Isopycnic centrifugation

A modified protocol of Manefield *et al.* (2002) was used to separate and analyze ^{13}C-enriched RNA. Density gradient centrifugation was performed in 2.0 ml polyallomer re-seal tubes in a S120VT vertical rotor (both Sorvall). Centrifugation was at 20 ºC for 48h at 64.000 r.p.m (150000 × *g*). Approximately 500 ng of total RNA was resolved in CsTFA gradients with an average of density 1.8 g ml^{-1}. Centrifugation media were prepared by mixing 1.86 ml of a 2.0 ± 0.5 g/ml CsTFA solution (Amersham Biosciences), 375 µl of RNAse free water (Fermentas) and 75 µl of deionized formamide (Promega). Control gradients were run with rRNA from unlabelled soil for each time course to calibrate the centrifugation system. A blank gradient, without RNA, was included with centrifugation for the range of expected buoyant densities. To obtain density fractions, a precisely controlled flow rate was achieved by displacing the gradient medium with RNAse free water at the top of the tube using an infusion syringe pump at flow rate of 100 µl min^{-1}. Centrifuged gradients were fractionated from bottom to top into 20 equal fractions (~100 µl per fraction). The density of each fraction was determined by weighing the fractions and by using an AR200 digital refractometer (Reichert Inc., Depew, NY, USA). RNA was

subsequently isolated from gradient fractions by precipitation with RNAse free isopropanol (Sigma). Each gradient fraction was checked for the presence of RNA by agarose gel electrophoresis and RNA quantified with a ND-1000 spectrophotometer.

Synthesis of cDNA and Domain-specific PCR quantification of density-resolved 16S and 18S rRNA

RNA samples from equilibrium density gradient fractions were reverse transcribed using Moloney Murine Leukemia Virus reverse transcriptase with low RNAse H activity (200 u/µl, ReverseAid^{TM} M-MuLVRT, Fermentas) using random hexaminer primers (0.2 µg/µl) according to the manufacture's protocol (RevertAid^{TM} First Strand cDNA Synthesis Kit, Fermentas). The reaction mixture (20 µl) contained 10 µl of 1:20-diluted template RNA. The cDNA produced was then quantified for bacterial 16S rRNA and fungal 18S rRNA genes by real-time PCR using the ABsolute QPCR SYBR green mix (AbGene, Epsom, UK) on a Rotor-Gene 3000 (Corbett Research, Sydney, Australia). All mixes were made using a CAS-1200 pipetting robot (Corbett Research, Sydney, Australia). Quantification of fungal and bacterial SSU ribosomal RNA gene copies in rhizosphere soil was carried as described in chapter 3. All the samples, and all standards, were assessed in at least two different runs to confirm the reproducibility of the quantification.

Community analyses by 16S and 18S rRNA-based PCR-DGGE analysis

PCR-Denaturing Gradient Gel Electrophoresis (PCR-DGGE) analysis of bacterial, fungal, *Pseudomonas* sp., *Burkholderia* ssp. and AMF communities of reverse transcribed density-resolved RNA fractions was performed with the primers, thermocycling regimes, and electrophoresis conditions previously described in chapters 3 and 4. Each density-resolved fraction was assessed in at least two different runs to confirm the reproducibility of the DGGE fingerprint across gels. The DGGE fingerprinting was binary coded and used in statistical analysis as "species" presence-absence matrices. The influence of CO_2 concentrations (ambient versus elevated), as examined by PCR-DGGE, was tested by distance-based redundancy analysis (db-RDA, Legendre & Anderson 1999). Jaccard's coefficients of similarity were first calculated between samples and used to compute principal coordinates (PCoA) in the R-package (Casgrain & Legendre 2001). When necessary, eigenvectors were corrected for negative eigenvalues using the procedure of Lingoes (1971) and all PCoA axes were then exported to Canoco version 4.5 (Ter Braak and Šmilauer, 2002) and treated as "species" data. To test the effects of the elevated CO_2 concentration and time of harvesting, these were entered as dummy binary-variables. In Canoco, the CO_2 concentrations factors were entered as the explaining variables in the model, while the time of harvesting was entered as a covariable. The significance of these models was tested with a Monte-Carlo test based on 999 permutations restricted for split-plot design, with whole-plots being the CO_2 flow cabinets. Further db-RDA analyses were also performed as above but on subsets of the whole dataset, by analyzing either plants species.

Cloning and sequencing of amplicons

PCR products using environment nucleic acid extractions or excised DGGE bands were obtained using several primer combinations as obtained in chapters 3 and 4 (see above). PCR products were purified with the High-Pure PCR product purification kit (Boehringer Mannheim, Almere, NL) and cloned into the pGEM-T Easy vector (Promega, Leiden, NL) according to the manufacturer's instructions. Plasmid extraction was performed using the Wizard Plus SV miniprep DNA purification kit (Promega, Benelux). Several clones with confirmed inserts of the expected size, were selected randomly for sequencing, using the vector –encoded universal T7 primer, from the bacterial-, fungal-specific, *Pseudomonas*-, *Burkholderia*- and AMF specific libraries (Table 1; Macrogen; South Korea). To confirm reliability of sequences derived from DGGE bands, three different colonies with the expected insert were sequenced per excised band. Sequences were aligned in the Bioedit Sequence Alignment Editor program (www.mbio.ncsu.edu/BioEdit/bioedit.html). To identify chimeric sequences in the clone libraries all recovered sequences were checked by using CHIMERA_CHECK 2.7 (Ribosomal Database Project II; http://rdp.cme.msu.edu).

Table 1. Primers, type of analyses, clone source and species detection.

Primers	Types of analyses	Clones sources (number)		Detection of	Reference
		PCR	DGGE bands		
968-gc/1378	DGGE gradient[2] (45-65% denaturant)	200[1]	-	Bacteria	Heuer *et al*. (1997)
Ba519f/Ba907r	real-time PCR				Luedres *et al*. (2004)
FR1-gc/FF390	DGGE gradient[2] (40-55% denaturant)	200[1]	40[1]	Fungi	(Vainio and Hantula 2000) (Lueders et al. 2004)
Fung5f/FF390r	real-time PCR				
Burk3/1378	DGGE gradient[2] (50-60% denaturant)	50[1]	22[1]	*Burkholderia* spp.	Salles *et al.* 2002
Burk3-GC/BurkR					
PsF/PsR	DGGE gradient[2] (45-65% denaturant)	50[1]	16[1]	*Pseudomonas* spp.	Widmer *et al* (1998)
968-gc/PsR					Garbeva *et al*. (2004)
LR1/FLR2	DGGE gradient[2] (20-55% denaturant)	50[1]	12[1]	AMF	Trouvelot *et al.* (1999)
FLR4-gc /FLR3					Van Tuinen *et al.* (1998) Golotte *et al.* (2004)

[1] PCR products and DGGE bands excised were selected respectively half for the 'heavy' and half from the 'light' density separated RNA fractions clone libraries.
[2] 100% denaturant is defined as 40% (v/v) formamide and 7 M urea

All cloned bacterial (~900 bp), *Pseudomonas* (~250bp*)* and *Burkholderia* (~ 500 bp) 16S rRNA gene sequences and fungal (~600 bp), AMF (~400 bp) 18S rRNA gene sequences were compared at the species level with sequences of public databases by using NCBI Blast (http://www.ncbi.nlm.nih.gov/blast).The bacterial clone sequences were compared at the family level with the sequences of the Ribosomal Database Project II Classifier (http://rdp.cme.msu.edu). To estimate the probability of observing differences in the frequency between libraries recovered from ambient and elevated CO_2 treatments, the cloned sequences were compared by the classification and library compare algorithm published in naïve Bayesian Classifier for Rapid Assignment of rRNA Sequences (Ribosomal Database Project II).

Results

Nucleic acid distributions in centrifugation gradients

At the end of the ^{13}C-CO_2 pulse labelling (day1, Fig 1 B and B1), the rRNA gradient profile of the bacterial and fungal community showed a pronounced peak in the 'heavy' rRNA fractions detected at densities >1.80 g/ml. The total fungal 18S rRNA templates amounted to ~70% of the bacterial rRNA quantities detectable, whereas the total amount of fungal 18S rRNA 'heavy' templates was proportionally higher than the bacterial 16S rRNA 'heavy' templates after 1 and 3 days (Fig 1 C and C1) post-labelling, indicating greater accumulation of ^{13}C in the fungal community as compared to the bacterial community at elevated CO_2 for these sampling times.
After 6 days (Fig 1 D and D1) post-labelling, a consistent decrease of 18S rRNA fungal target molecules in the 'heavy fractions' was detected at ambient and elevated CO_2, whereas an increase of 16S rRNA bacterial target molecules in the 'heavy' fractions was observed at elevated CO_2. These contrasting patterns persisted throughout the last two sampling times, with slightly less pronounced peaks of the 'heavy' fractions in both communities (day 14, Fig 1 E, E1 and day 21, Fig 1 F, F1).

Microbial incorporation of ^{13}C labelled substrates

It was determined that the 'heavy' RNA fractions localized within a buoyant of density zone between 1.80 g ml^{-1} and 1.84 g ml^{-1} CsTFA, with 'light' fractions between 1.74 g ml^{-1} to 1.79 g ml^{-1} CsTFA (Fig. 1). Based upon the real-time PCR results, typical 'heavy' fractions were selected for subsequent reverse transcription polymerase chain reaction (RT-PCR) denaturing gradient gel electrophoresis (DGGE) analysis. In addition, 'light' fraction were included in the analyses to allow comparison with the community not incorporating a significant amount of plant-derived ^{13}C. As controls, the PCR-DGGE profiles of the unlabelled rhizosphere material (previous labelling, day 0) were also checked for 16S rRNA and 18S rRNA using a appropriate primers, verifying the absence of low buoyancy ('heavy') RNA from unlabeled samples.
The ^{12}C-RNA fractions using bacterial, *Pseudomonas* (Fig. 2A) and *Burkholderia* specific primer sets (Fig. 2B) showed that the community compositions were strongly influenced by elevated CO_2 ($P < 0.001$). The ^{13}C-RNA-based DGGE banding patterns of the bacterial, *Pseudomonas* (Fig. 2A) and *Burkholderia* (Fig. 2B) communities under elevated CO_2 were significantly different ($P < 0.001$) from the ambient CO_2 ones across the entire time course. Within each community only few bands were labelled at day 1 with band numbers increasing through the day 21.At the end of the harvesting procedure (day 21), the bacterial and *Pseudomonas* communities were entirely labelled, showing a fingerprinting profile similar to the 'light' fraction. An exception was represented by *Burkholderia* in which the incorporation pattern changed significantly only in day 1, 6 and 21 and in contrast to the other groups labelled C was not distributed over the entire *Burkholderia* community.

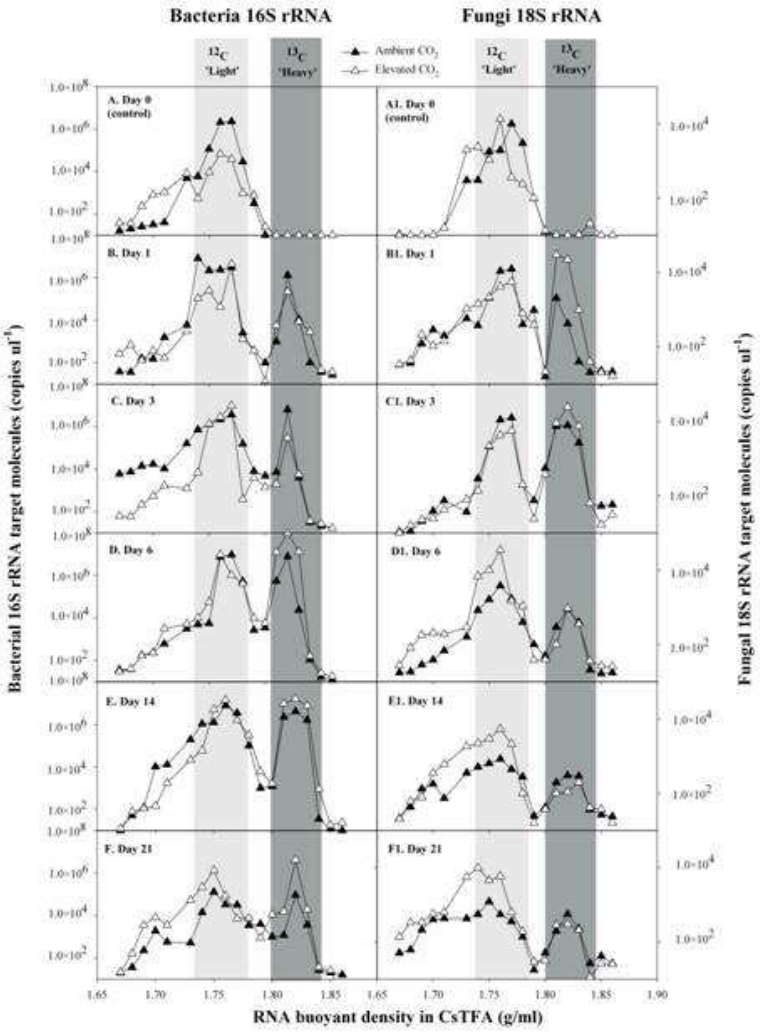

Figure 1: CsTFA density gradient centrifugation of rRNA extracted from *F. rubra* rhizosphere soil at ambient (black triangles) and elevated CO_2 (white triangles) conditions at day 0 (A, A1; unlabelled control), and day 1 (B, B1), 3 (C, C1), 6 (D, D1), 14 (F, F1) and 21(E, E1) after the incubation with ^{13}C-CO_2. Bacterial and fungal SSU rRNA template distribution within gradient fractions was quantified with 'real-time' RT-PCR. The density-range characteristic for the 'light' ^{12}C-rRNA is shaded in light grey and for the 'heavy' ^{13}C-rRNA in dark grey. All the density separated fractions were used for the PCR-DGGE fingerprinting analysis. The fractions from which the clone libraries of selected templates were generated are included in the light grey and dark grey shaded areas.

The ^{12}C-fungal DGGE profiles (Fig. 2C) were significantly affected by elevated CO_2 ($P < 0.001$). Along the different time courses (day 0, 1, 3, 6, 14, 21), few not significant ($P = 0.85$) changes in the fractions taken along the ^{13}C gradient were detected. In contrast to bacterial ^{13}C-based community profiles, no significant changes were observed along the course of the time series ($P = 0.4$). Thus, most populations that received label during the experiment were already labeled within one day after the ^{13}C pulse.
The AMF-specific DGGE profiles generated from ambient and elevated CO_2 rhizosphere samples showed significantly different fingerprinting patterns ($P < 0.001$; Fig. 2D). The 'heavy' AMF RNA clearly corresponded to a subset of the diversity found in the light RNA and DNA.

Identification of populations recovered by community profiling

Specific microbial community members represented by the PCR-DGGE bands within the 'light' and 'heavy' RNA-based profiles were subsequently identified by cloning and sequencing. To facilitate the identification of PCR-DGGE bands, various specific clone libraries were constructed from the ^{12}C- and ^{13}C-centrifugation gradient fractions (Fig. 3 and Table 1, 2) per analysed microbial community (bacteria, *Pseudomonas*, *Burkholderia*, fungi and AMF), sampling time (days 0, 1, 3, 6, 14 and 21) and CO_2 condition (ambient and elevated CO_2) (Table 1). By using a Bayesian estimator of the diversity for non-invasive sampling of the different phylotypes affiliated with the different communities, we observed that we did not underestimate due to under-sampling the diversity of fungi, AMF, bacteria, *Pseudomonas* and *Burkholderia*, communities (Petit & Valiere, 2006). Significant difference ($P < 0.001$) generated by comparing the 'light' and 'heavy' clone libraries at ambient and elevated CO_2 were confirmed by using naïve Bayesian Classifier for Rapid Assignment of rRNA Sequences (Ribosomal Database Project II). In all the libraries analysed, the 'heavy' RNA represented a subset of the diversity found in the 'light' RNA.

Fungal community analyses

The analysis of 100 fungal cloned sequences in the ambient CO_2 'light' clone library (Laf) showed that 77% were affiliated to Ascomycota and 23% belonged to Glomeromycota (Fig.3 and Table 2). Sequence recovery in the elevated CO_2 'light' clone library (Lef) showed 70% as affiliated with Ascomycota, 26% Glomeromycota and the remaining 4% to Basidiomycota.Within the 'heavy' ambient and elevated CO_2 18S rRNA clone libraries (Haf and Hef) all the Glomeromycota-likes sequences recovered from AMF-specific analysis were affilaited with *Glomus* in the Hef library and *Acaulospora* species in Haf. ~50% of them were affiliated 100% to *Glomus claroideum* and *Acaulospora lacunosa* respectively one at elevated and the other at ambient atmospheric CO_2 (Fig 2d, Fig. 3 and Table 2). The other 50% of AMF sequences were also related to recognize *Glomus* and *Acaulospora* group respectively at elevated and ambient CO_2. 24 Hours post pulse labeling 50% of the sequences were affiliated to *Glomus* species decreasing to 36% at day 21 at elevated CO_2. At ambient CO_2 36% of the sequences were affiliated to *Acaulospora* species at day 1 decreasing to 16% at day 21.

Table 2 .Characterization of direct cloning of 16S rRNA and 18S rRNA PCR products from the light (^{12}C-RNA) and heavy (^{13}C-RNA) clone libraries at ambient and elevated atmospheric CO_2 conditions. From the 18S rRNA clone libraries more than 50 randomly chosen clones were sequenced, from the 16S rRNA clone library more than 100 clones were selected. Accession numbers of the sequences are indicated after the affiliation group. An asterisks was added next to the ascension number when sequences where retrieved either from bands of the ^{12}C/^{13}C-RNA-based denaturing gradient gel electrophoresis (DGGE) and RNA clone libraries (see Table 1). + refer to the presence of sequences and – to their absence in the different treatments. The numbers stated in parenthesis refer to the bands excised from the DGGE analysis and indicated in figure 2. The taxonomic affiliation is according the RDP classifier system, and the sequences closest neighbours in the GenBank database.

Identity (PHYLUM, family)	Ambient CO_2						Elevated CO_2						Genera (accession no./ % identity)
	^{12}C-RNA	^{13}C-RNA clone library					^{12}C-RNA	^{13}C-RNA clone library					
	t = 0	1 d	3 d	6 d	14 d	21 d	t = 0	1 d	3 d	6 d	14 d	21 d	
Glomeromycota	- (1)	-	-	-	-	-	+	+	+	+	+	+	*Glomus claroideum (AY639288/100%) (*)*
Glomeraceae													
Glomeromycota	+ (2)	+	+	+	+	+	+	-	-	-	-	-	*Acaulospora lacunose (AJ5102301/100%) (*)*
Acaulosporaceae													
Ascomycota	+ (17)	+	+	+	+	+	+	+	+	+	+	+	*Hyphodiscus hymeniophilus (DQ227258/99%) (*)*
Hyaloscyphaceae													
Ascomycota	+ (18)	+	+	+	+	+	+	+	+	+	+	+	*Tolypocladium cylindrosporum (AB208110/100%) (*)*
Clavicipitaceae													
Ascomycota	+ (19)	-	-	+	+	+	+	-	-	+	+	+	*Cordyceps cylindrical (AY526490/100%) (*)*
Clavicipitaceae													
Ascomycota	+ (20)	+	+	+	+	+	+	+	+	+	+	+	*Aspergillus niger (EU159262/100%) (*)*
Trichocomaceae													
Ascomycota	+ (22)	+	+	+	+	+	-	-	-	-	-	-	*Trichoderma harzianum (EF672343/100%) (*)*
Hypocreaceae													
Ascomycota	+ (23)	+	+	+	+	+	+	+	+	+	+	+	*Phialocephala sphaeroides (AY524844/99%) (*)*
Helotiales													
Ascomycota	-	-	-	-	-	-	+ (15)	-	-	+	+	+	*Capnobotryella sp. (AJ972860/100%) (*)*
Ascomycota	-	-	-	-	-	-	+ (16)	-	-	+	+	+	*Heteroconium chaetospira (DQ521605/99%) (*)*
Herpotrichiellaceae													
Basidiomycota	-	-	-	-	-	-	+ (24)	+	+	+	+	+	*Trichosporon porosum (AB051045/99%) (*)*

Identity (PHYLUM, family)	Ambient CO_2						Elevated CO_2						Genera (accession no./ % identity)
	^{12}C-RNA	^{13}C-RNA clone library					^{12}C-RNA	^{13}C-RNA clone library					
	t = 0	1 d	3 d	6 d	14 d	21 d	t = 0	1 d	3 d	6 d	14 d	21 d	
Apicomplexa	+ (21)	-	-	+	+	+	-	-	-	-	-	-	*Eimeriidae (EF024025/100%) (*)*
Eimeriidae													
Uncultured fungus	+ (25)	+	+	+	+	+	-	-	-	-	-	-	*(AY605199/97%) (*)*
Proteobacteria Pseudomonadaceae	+ (3)	+	+	+	+	+	+	+	+	+	+	+	*Pseudomonas fluorescens (EF528294/100%) (*)*
	+ (4)	-	-	-	-	-	+	-	+	+	+	+	*Pseudomonas aeruginosa (EU131096/100%) (*)*
	+ (5)	-	-	-	-	-	+	+	+	+	+	+	*Pseudomonas trivialis (AM900687/100%) (*)*
	+ (6)	-	-	-	-	-	+	+	+	+	+	+	*Pseudomonas putida (EU179737/100%) (*)*
Proteobacteria Bradyrhizobiaceae	- (7)	-	-	-	-	-	+	+	+	+	+	+	*Bradyrhizobium japonicum (CP000463/100%) (*)*
Proteobacteria Burkholderiaceae	+ (8)	+	+	+	+	+	+	+	+	+	+	+	*Burkholderia phenazinium (AM502990/100%) (*)*
	+ (9)	+	-	-	-	-	+	+	+	+	-	-	*Burkholderia fungorum (EF65001/99%) (*)*
	+ (10)	+	+	+	+	+	+	+	+	+	-	-	*Burkholderia xenovorans (EF467847/99%) (*)*
	+ (11)	+	+	+	-	-	+	-	-	+	+	+	*2,4-D-degrading bacterium (AF184931/99%) (*)*
	+ (12)	-	-	-	-	-	+	+	+	+	+	+	*Burkholderia cepacia (AY741358/98%) (*)*
	+ (13)	-	-	-	-	-	+	-	-	+	+	+	*Burkholderia glathei (AY154379V/99%) (*)*
	+ (14)	-	-	+	+	+	+	-	-	-	-	-	*Burkholderia phytofirmans (AY497470/100%) (*)*
Proteobacteria	+	+	+	+	+	+	-	-	-	-	-	-	*Xanthobacter flavus (EF592179/96%)*
Xanthobacteraceae													
Proteobacteria	+	-	-	+	+	+	-	-	-	-	-	-	*Unclassified Magnetospirillum (95%)*
Rhodospirillaceae													
Proteobacteria	+	+	+	+	+	+	+	+	+	+	+	+	*Unclassified rhizobiales (95%)*
Rhizobiales													
Proteobacteria	+	-	-	-	-	-	+	-	-	-	-	-	*Unclassified actinomycetales (100%)*
Acetobacteraceae													
Proteobacteria	+	-	-	+	+	+	-	-	-	-	-	-	*Unclassified Enterobacteriaceae (86%)*
Enterobacteriaceae													
Proteobacteria	-	-	-	-	-	-	+	+	+	+	+	+	*Unclassified Geobacteraceae (98%)*
Geobacteraceae													
Unclassified Proteobacteria	+	+	+	+	+	+	+	+	+	+	+	+	
Chloroflexi	+	+	+	+	+	+	-	-	-	-	-	-	*Unclassified Caldilineacea (95%)*
Chloroflexaceae													
Planctomycetes	+	+	+	+	+	+	-	-	-	-	-	-	*Unclassified Gemmata (100%)*
Planctomycetaceae													

Identity (PHYLUM, family)	Ambient CO_2						Elevated CO_2						Genera (accession no./ % identity)
	^{12}C-RNA	^{13}C-RNA clone library					^{12}C-RNA	^{13}C-RNA clone library					
	t = 0	1 d	3 d	6 d	14 d	21 d	t = 0	1 d	3 d	6 d	14 d	21 d	
Actinobacteria	+	-	-	-	-	-	+	-	-	-	-	-	*Unclassified actinomycetales (100%)*
Actinomycetales													
Verrucomicrobia	+	-	-	-	-	+	-	-	-	-	-	-	*Subdivision 3 Genera incertae sedis (98%)*
Subdivision 3													
Firmicutes	+	-	-	-	-	-	+	-	-	-	-	-	*Unclassified Desulfitobacterium (95%)*
Peptococcaceae													
Firmicutes	+	-	-	-	-	-	+	-	-	-	-	-	*Unclassified Bacillus sp.(95%)*
Bacillaceae													

Table 2 (Continuation) .Characterization of direct cloning of 16S rRNA and 18S rRNA PCR products from the light (^{12}C-RNA) and heavy (^{13}C-RNA) clone libraries at ambient and elevated atmospheric CO_2 conditions. From the 18S rRNA clone libraries more than 50 randomly chosen clones were sequenced, from the 16S rRNA clone library more than 100 clones were selected. Accession numbers of the sequences are indicated after the affiliation group. An asterisks was added next to the ascension number when sequences where retrieved either from bands of the ^{12}C/^{13}C-RNA-based denaturing gradient gel electrophoresis (DGGE) and RNA clone libraries (see Table 1). + refer to the presence of sequences and – to their absence in the different treatments. The numbers stated in parenthesis refer to the bands excised from the DGGE analysis and indicated in figure 2. The taxonomic affiliation is according the RDP classifier system, and the sequences closest neighbours in the GenBank database.

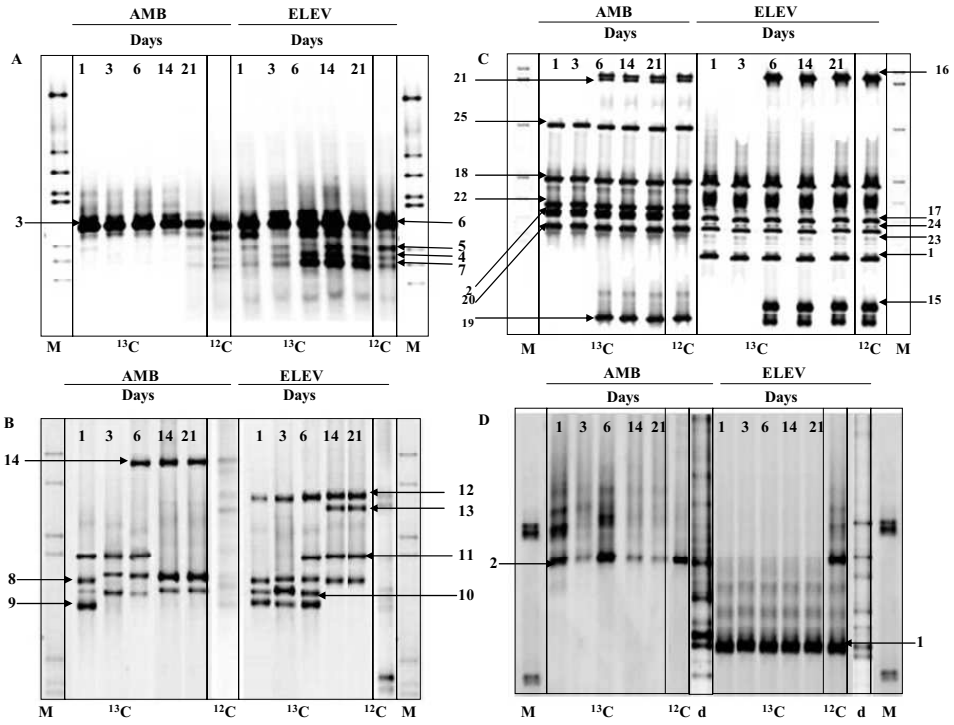

Figure 2: Denaturing gradient gel electrophoresis banding pattern of (A) Pseudomonas, (B) Burkholderia, (C) fungal and (D) AMF SSU RNA partial sequences of the density resolved fractions at buoyant of density banding at 1.82 g/ml for the 'heavy fractions' at ambient (AMB) and elevated (ELEV) CO_2 at day 1, 3, 6, 14 and 21 after the incubation with ^{13}C-CO_2. The density resolved 'light fraction' fraction at buoyant of density banding at 1.76 g/ml at day 0 was selected as representative since the community fingerprinting profiles of the different light fractions were not significantly affected by the time of harvesting. The DNA fingerprinting profile (d) is added as representative of the overall AMF fungal community at ambient and elevated CO_2. The number refer to the characterization of direct cloning of 16S rRNA and 18S rRNA PCR products from the light (^{12}C-RNA) and heavy (^{13}C-RNA) clone libraries at ambient and elevated atmospheric CO_2 conditions (Table 2).

The remaining clones were affiliated to *Ascomycota* only at ambient CO_2 and to *Ascomycota* and *Basidiomycota,* namely *Trichosporum porosum* at elevated CO_2. In the Haf *Trichosporum porosum, Capnobotrytella, Heteroconicum chaetospira*-like sequences were not detected, yet the *Tricoderma harzianum, Eimeriidae*-like sequences and unidentified fungal population were recovered at ambient CO_2 (Fig 2C, Table 2). The sequences data derived from the PCR-DGGE bands products specific for Fungi and AMF allowed us to identify the fungal populations that utilized plant derived ^{13}C at ambient and elevated CO_2 across the different sampling times and these sequences were affiliated to the

same species of AMF and fungi revealed by the PCR-cloning strategy described above (Fig. 2C, 2D; Table 1).

Bacterial community analyses

The analysis of 100 bacterial clone sequences in the 'light' clone ambient CO_2 library (Lab) revealed that 74 % were affiliated to Proteobacteria and the remaining 26 % belonged to diverse phylogenetic groups including *Chloroflexi*, *Planctomycetes* and *Verrucomicrobia* (Fig. 3 and Table 2). At elevated CO_2 all recovered sequences affiliated with Proteobacteria along the different sampling times (Fig 3 and Table 2). In the 'heavy' ambient 16S rRNA clone library (Hab) 24 hours post-pulse labeling 57% of the sequences were affiliated with the *Proteobacteria* increasing to up 90% at day 6 and staying stable at ~ 73% at day 14 and 21. The remaining clones were affiliated to *Chloroflexi*, *Planctomycetes* and *Verrucomicrobia*. The *Verrucomicrobia* population appeared to incorporate ^{13}C only at day 21. In contrast, all 'heavy' 16S rRNA clone sequences at elevated CO_2 (Heb) were affiliated with Proteobacteria at all sampling times. Within the Proteobacteria, significant differences ($P < 0.001$) were detected when comparing Hab and Heb libraries using a naïve Bayesian Classifier for Rapid Assignment of rRNA Sequences (Ribosomal Database Project II). In the Heb library, we detected Geobacteraceae and Bradyrhizobiaceae, whereas in the Hab Xanthobacteraceae, Rhodospirillaceae and Enterobacteriaceae-like sequences were not detected (Table 2 and Fig. 3).
The frequency and diversity of the sequences affiliated with the Burkholderiaceae and Pseudomonaceae at the species level showed higher variability in Hab than in the Heb library (Fig. 3). The sequence data derived from the PCR-DGGE bands of the density separated gradient fractions specific for *Burkholderia* and *Pseudomonas* allowed us to identify the specific populations using and incorporating ^{13}C-exudates at ambient and elevated CO_2 (Fig. 2A, 2B). Over time the diversity of the active ^{13}C-Burkholderiaceae community differed at elevated CO_2 conditions. *B. fungorum*, *B. cepacia* and *B. glathei* community were present under elevated CO_2 together with *B. phenazinum, B xenoforans* and *2, 4-D–degrading bacterium* (belonging to the Burkholderiaceae family) - species that were also active at ambient CO_2. At ambient CO_2 *Pseudomonas fluorescens* was identified as the only dominant *Pseudomonas*-like sequence detected at all sampling times. At elevated CO_2, the biodiversity of *Pseudomonas*–like sequences visibly increased, new active species were identified along the different time courses, such as *P. aeruginosa, P. trivialis* and *P. putida.*

Discussion

We previously described (see chapter 5) that the main response to increased translocation of C at elevated CO_2 conditions proceed via AMF, which rapidly accumulate plant–assimilated C that is subsequently gradually released to rhizo-competent bacterial populations in soil (Olsson & Johnson 2005; Jones *et al.* 2004). Here, we demonstrated a pronounced shift in the AMF community under elevated atmospheric CO_2 conditions. At current atmospheric CO_2 levels, an *Acualosporaceae* dominated population were the main utilizers of root derived C and at elevated CO_2 *Glomeraceae* dominated in ^{13}C incorporation. This shift in the active AMF community may be associated with major changes in the associated ^{13}C-substrates incorporating microbial community altering rhizosphere plant-microbial interactions under elevated CO_2. Different AMF families have

been demonstrated to utilize different life-history strategies and occupying distinct niches (Cavender-Bares *et al.* 2004). So, also *Acaulosporaceae* and *Glomeraceae* are recognized to have different niches requirements and life histories (Maherali & Klironomos, 2007) Our results are in accordance with previous field and glasshouse CO_2 treatment studies, in which *Glomus* species were recognized to be dominant at elevated CO_2 (Klironomos *et al.* 2005; Staddon *et al.* 2004; Gamper *et al*. 2005; Heinemeyer *et al*. 2006) due to superior competitive ability for root derived substrates (Vandenkoornhuyse *et al.* 2007). Thus, we may exclude that the observed shift in the AMF community is due to a methodological bias as recently shown by Vandenkoornhuyse *et al.* 2007. Indeed, our analysis was not only based on AMF-specific primers, which may miss some taxa, but results were also confirmed by broad fungal-specific analysis. Moreover, our results agree with Klironomos *et al.* (2005) as the central role of mycorrhizae in the elevated CO_2 belowground C-pathway was shifted from *Acaulosporaceae* to *Glomeraceae* without changing in magnitude. Hence, we hypothesize that the shift in dominant populations of AMF under elevated CO_2 may consequently induce profound shifts in rhizobacterial communities. For example, shifts in active AMF taxa due to increased level of atmospheric CO_2 could affect microbial community composition of active root-inhabiting microbes by retaining C photosynthetate in mycorrhizal biomass thereby controlling its time of release to soil microbial community (see chapter 5), by modifyng rhizodeposition quality and by affecting the physical and chemical conditions of the adjacent soil (see chapter 3 and 4).

Major changes were also observed in the fungal and bacterial community structure as well as in the richness of active species. Under elevated CO_2 conditions the fungal community had an increase of sequences affiliated to the *Basidiomycota* phylum. At elevated CO_2, the ^{13}C-incorporating bacterial community was represented only by Proteobacteria species. Within the Proteobacteria, the frequency and diversity of the sequences affiliated with the Pseudomonaceae and Burkholderiaceae were highly variable (Fig. 2 and 3). At ambient CO_2, *P. fluorescens* was the main species benefiting from root exudates. Under elevated CO_2 conditions, the diversity of the *Pseudomonas* populations incorporating plant-derived C increased over time with the recovery of *P. fluorescens*, *P. aeruginosa, P. trivialis,* and *P. putida*- sequences. *The species richness of Burkholderiaceae under elevated CO_2 increased by the presence of B. fungorum*, *B. cepacia* and *B. glathei* together with *B. phenazinum, B. xenoforans* and *2, 4–degrading bacterium* species already active at ambient CO_2. Interestingly, Pseudomonaceae, such as *P. fluorescens*, *P. aeruginosa* and *P. putida,* the Burkholderiaceae and *Bradyrhizobium japonicum* (Table 2) species reported under elevated CO_2 atmospheric conditions in this study are recognized to be mycorrhizal helper bacteria (MHB) *associated with* Glomus *species* (Frey-Klett *et al.* 2007). *One possible explanation of the presence of active MHB bacteria under elevated CO_2 could be the production by AMF of the disaccharide* trehalose. Previous studies have shown that mycorrhizal fungi receive up to the 30% of the total fixed carbon, under current atmospheric conditions. A large proportion of this carbon is subsequently transformed into trehalose, which can exert strong selection on bacterial communities in the mycorrhizosphere, including potential MHB strains, such as *Pseudomonas*, *Burkholderia* and *Bradyrhizobioum* species (reviewed in Frey-Klett *et al.* 2007). Interestingly, we found that the amount of trehalose produced in the mycorhizosphere was 4 time higher at elevated CO_2 versus ambient CO_2 concentrations.

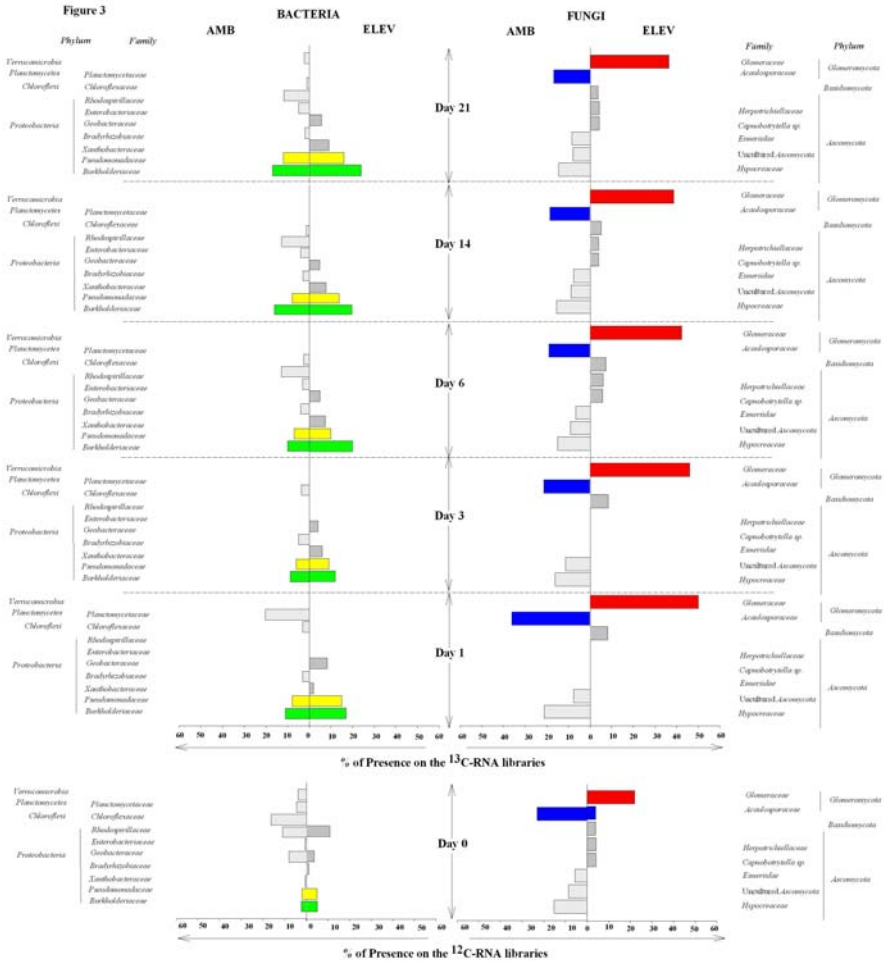

Figure 3: Relative distribution of taxa that showed significant differences in frequency when comparing 'light' (^{12}C) and 'heavy' (^{13}C) 16S rRNA and 18S rRNA clone libraries, compared at the family level using the Ribosomal Database Project II Classifier (http://rdp.cme.msu.edu) at ambient (AMB) and elevated (ELEV) CO_2 conditions at day 0 (unlabelled control), 1, 3, 6, 14 and 21 after the incubation with ^{13}C-CO_2. Bacterial and fungal libraries generated by the cloned sequences were compared by the classification and library compare algorithm published in naïve Bayesian Classifier for Rapid Assignment of rRNA Sequences (Ribosomal Database Project II). In green and yellow, the Proteobacteria families with the highest variability at species level in both CO_2 treatments, respectively Burkholderiaceae and Pseudomonaceacea, and, in blue and red, the most affected AMF families, Acaulosporaceae and Glomeraceae, respectively.

Our findings demonstrate that highly distinct microbial communities incorporate plant-derived C under elevated versus ambient atmospheric CO_2 conditions. Arbuscular mycorrhizal fungi (AMF) seem to play a central role in these dynamics. Shifts in AMF communities, toward dominance by opportunistic *Glomus*, displacing resident *Acaulospora* populations, may have a dramatic effect on shaping associated microbial communities. These potential changes in species assemblages could affect soil carbon dynamics and, consequently, the feedback effects of terrestrial soil-vegetation systems on global environmental change. To date, most studies addressing the effects of increased CO_2 on the plant-microbial interactions have generally emphasized either the importance of enhanced C-input for the microbial biomass and activity or the increased C allocation to mycorrhizal fungi and root exudation (Staddon, 2005; Phillips, 2007). Little attention has been directed to connecting the effects of elevated CO_2 with the pathway of C input to the soil via mycorrhizal associations and with its subsequent effect on the structure of active root-associated communities. Our results demonstrate the importance of mycorrhizal fungi and specific rhizosphere bacteria in terrestrial C fluxes, as previously suggested (Staddon, 2005, Chapter 5), thereby emphasizing the need to understand the dynamics of these organisms when assessing the current, and predicted future, effects of rising atmospheric CO_2 concentrations. We therefore provide new evidence of a central role of active root inhabiting microorganism in mediating potential impacts of elevated CO_2 in plant-soil systems and the global C cycle.

Acknoledgments

Thanks to Robert Griffiths and Bruce Thomson (CEH, Oxford, UK) for introduction to the SIP technique. We extend our gratitude to Caroline Plugge at the Wageningen University (NL). This study was supported by a Netherlands Research Council (NWO) grant of the Biodiversity and Global Change program awarded to J.A. van Veen (852.00.40) and the NWO-VIDI grant to H.T.S. Boschker.